AIP | Applied Physics Letters

Dynamically tunable broadband mid-infrared cross polarization converter based on graphene metamaterial

Hua Cheng, Shuqi Chen, Ping Yu, Jianxiong Li, Boyang Xie et al.

Citation: Appl. Phys. Lett. **103**, 223102 (2013); doi: 10.1063/1.4833757
View online: http://dx.doi.org/10.1063/1.4833757
View Table of Contents: http://apl.aip.org/resource/1/APPLAB/v103/i22
Published by the AIP Publishing LLC.

Dynamically tunable broadband mid-infrared cross polarization converter based on graphene metamaterial

Hua Cheng, Shuqi Chen,[a] Ping Yu, Jianxiong Li, Boyang Xie, Zhancheng Li, and Jianguo Tian[a]
The Key Laboratory of Weak Light Nonlinear Photonics, Ministry of Education, School of Physics and TEDA Applied Physics School, Nankai University, Tianjin 300071, China

(Received 1 October 2013; accepted 10 November 2013; published online 25 November 2013)

We present a mid-IR highly wavelength-tunable broadband cross polarization conversion composed of a single patterned top layer with *L*-shaped graphene nanostructures, a dielectric spacer, and a gold plane layer. It can convert linearly polarized light to its cross polarization in the reflection mode. The polarization conversion can be dynamically tuned and realize a broadband effect by varying the Fermi energy without reoptimizing and refabricating the nanostructures. This offers a further step in developing the tunable polarizers and the polarization switchers. [http://dx.doi.org/10.1063/1.4833757]

Optical activity, which was defined as the rotation of polarization of light after passing through circularly birefringent materials, has now been widely used in many areas like optics, analytical chemistry, and molecular biology.[1] The recently emerging concept of metamaterials opens up the possibility to enhance and expand optical activity effects, surpassing that of natural birefringent and chiral materials. Especially, through specific structural and material design, a near-complete cross polarization conversion (CPC) has been achieved with metamaterials, such as multilayered metasurfaces,[2–5] subwavelength metallic apertures,[6–8] and metallic cut wire arrays.[9] It is worth noting that most such CPC metamaterials are narrowband and may only be tuned to different wavebands by carefully reoptimizing the geometry parameters owing to the reliance on resonances, which limit their uses in practice. One way to overcome this limitation is to stack multilayer composite structures with different geometrical dimensions or orientations.[10–12] However, these designs need to precisely align between the layers, which complicate the fabrication process.

Another way to overcome this limitation is to use tunable metamaterials, which rely on integrating metamaterials with optically active materials such as liquid crystals,[13] semiconductors,[14] and nonlinear media.[15] The optical response of these metamaterials can be actively controlled by external stimulus, such as electric field, magnetic field, voltage, or temperature. Among all these techniques, voltage control is one of the simplest ways in practical operations. Single-layer graphene (SLG), whose conductivity can be dynamically controlled by electrostatic gating, seems to be a good candidate for designing tunable devices and becomes a hot material in both physics and engineering.[16–18] SLG can strongly interact with light over a wide frequency range, especially suited for the mid-IR frequency range because of the combination of its strong plasmonic response and negligible loss. Vakil and Engheta theoretically demonstrated that nonuniform conductivity patterns of graphene can be used as a platform for infrared metamaterials and transformation optical devices.[19] Mousavi *et al*. demonstrated that Fano resonant properties can be tuned by combining voltage-gated SLG and metamaterials together.[20] Fang *et al*. demonstrated the tunability and hybridization of plasmons in graphene nanostructures.[21] Recently, the metamaterials based on SLG have wildly been demonstrated to manipulate the polarization states of incident light in both theory[22,23] and experiment.[24,25] These studies open an exciting avenue towards designing voltage-controlled tunable metamaterials at mid-IR frequencies.

In this letter, we proposed a highly wavelength-tunable broadband CPC composed of a single patterned top layer with *L*-shaped graphene nanostructures, a dielectric spacer, and a gold plane layer in the mid-IR regime. We demonstrate that the designed CPC can convert linearly polarized light to its cross polarization in the reflection mode. Moreover, the polarization conversion can be dynamically tuned and realize a broadband effect by varying the Fermi energy without reoptimizing and refabricating the nanostructures, which offers possible applications as tunable polarizers and polarization switchers.

The schematic diagram of the *L*-shaped graphene metamaterial used in numerical simulations is shown in Fig. 1, with its geometrical parameters described in the caption. It contains an array of *L*-shaped SLG and a 100 nm thick gold board, which are separated by 1200 nm thick dielectric medium with the dielectric constant of 2.25. The optical constants of bulk gold in the infrared spectral regime are described by using the Drude model with the plasma frequency $\omega_p = 1.37 \times 10^{16}\,\mathrm{s}^{-1}$ and the damping constant $\omega_c = 4.08 \times 10^{13}\,\mathrm{s}^{-1}$.[26] The conductivity of graphene $\sigma(\omega) = \frac{e^2 E_F}{\pi\hbar^2}\frac{i}{\omega + i\tau^{-1}} + \frac{e^2}{4\hbar}\left[\theta(\hbar\omega - 2E_F) + \frac{i}{\pi}\left|\frac{\hbar\omega - 2E_F}{\hbar\omega + 2E_F}\right|\right]$ is computed within the local random phase approximation limit at the zero temperature.[27] The intrinsic relaxation time is expressed as $\tau = \mu E_F / e v_F^2$, where $v_F \approx c/300$ is the Fermi velocity and $\mu = 10000\ \mathrm{cm}^2/\mathrm{Vs}$ is the measured DC mobility.[28] The finite element method (FEM) based software of COMSOL Multiphysics[29] was used to design and optimize the tunable broadband CPC. In the simulation, a linearly polarized plane wave with *x* polarization is used as the excitation

[a]Authors to whom correspondence should be addressed. Electronic addresses: schen@nankai.edu.cn and jjtian@nankai.edu.cn

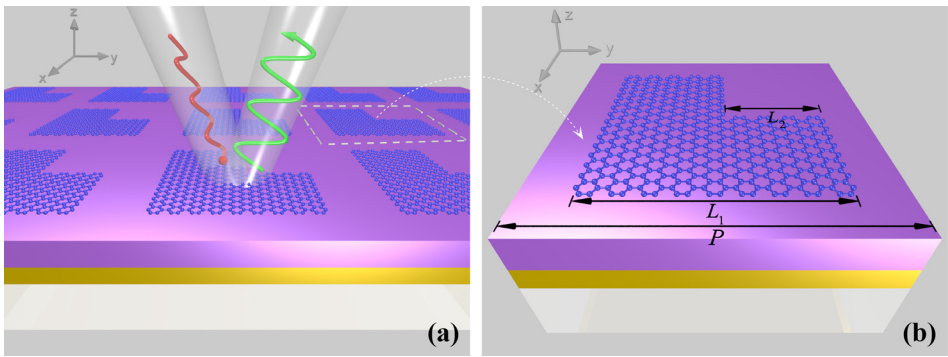

FIG. 1. (a) Schematic model of the designed CPC based on *L*-shaped graphene metamaterial and (b) unit cell nanostructure of our design: $L_1 = 100$ nm, $L_2 = 50$ nm, and the periodicity of $P = 150$ nm.

source, and periodic boundary conditions in all *x*-*z* and *y*-*z* planes are considered.

The designed CPC can work in the reflection mode as the transmission is suppressed by the ground gold plane. The polarized reflectances R_{xx} and R_{xy} (R_{ij} denotes *j*-polarized reflectance from *i*-polarized incidence) as a function of wavelength are shown in Fig. 2(a), where the Fermi energy is fixed as 0.9 eV. Strong polarization conversion is revealed as a reflection peak in R_{xy} at about 7.72 μm with a dip in R_{xx}, indicating an energy transferring from original polarization state to the orthogonal one with an almost 90° rotation. This remarkable characteristic can also be seen from the polarization conversion rate (PCR), which is defined as $\mathrm{PCR} = R_{xy}/(R_{xx} + R_{xy})$.[30] It is clearly found the maximum PCR reaches a high value of 0.98 at about 7.72 μm, as shown in Fig. 2(b). Besides the reflectance, FEM calculations can also provide us the information of reflection phase. The reflection phase difference for two polarizations as a function of wavelength is given in Fig. 2(c). The reflection phase difference approaches 0° at about 7.72 μm, indicating that a linearly polarization state can be realized. Furthermore, we employ the polarization azimuth angle θ, which is defined as $\theta = \frac{\pi}{2} + \frac{1}{2}\arctan[2|E_x||E_y|\cos\varphi/(|E_x|^2 - |E_y|^2)]$,[31] to describe the angle between the major polarization axis and the *x* axis. The values of $|E_x|$ and $|E_y|$ are proportional to the *x* and *y* polarized reflectance as shown in Fig. 2(a), and φ is the phase difference between the *y* and *x* components. The polarization azimuth angle θ as a function of wavelength is plotted in Fig. 2(d), which goes up to nearly 90° around the wavelength of 7.72 μm. The above results confirm the fact that a half wave plate with 90° polarization rotation is achieved by this graphene metamaterial at about the wavelength of 7.72 μm when the Fermi energy is 0.9 eV.

Compared with traditional metal plasmonics, the most important advantage for the graphene is the capability of dynamically tuning the conductivity through chemical or electrostatic gatings. To demonstrate the tunability of the polarization conversion, we calculated the amplitude ratio and phase difference between the *x* and *y* components of the reflectance as a function of Fermi energy and wavelength in Figs. 3(a) and 3(b), where the incident polarization is along *x* axis. Results clearly demonstrate that increasing Fermi energy can lead to a blue shift in the resonant wavelength and comparatively stronger amplitude ratio at the resonance wavelength, indicating the tunability of polarization conversion. This behavior can be interpreted by the resonance condition of $k_{spp} \simeq k_R \propto L_{eqv}$, where k_{spp} represents the wave vector of surface plasmon in graphene, k_R represents the resonant wave vector of incident light, and L_{eqv} represents the equivalent resonant length of *L*-shaped graphene nanostructure. Combining with the surface plasmon satisfied

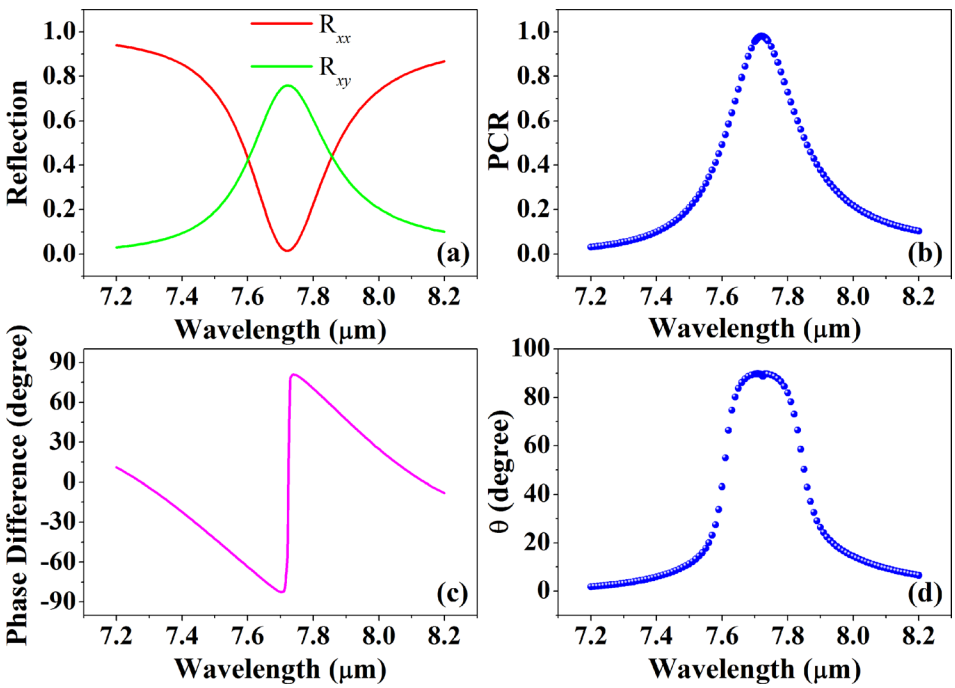

FIG. 2. (a) Calculated polarized reflectances R_{xx} and R_{xy}, (b) PCR, (c) reflection phase difference, and (d) polarization azimuth angle θ as a function of wavelength, where the Fermi energy is fixed at 0.9 eV.

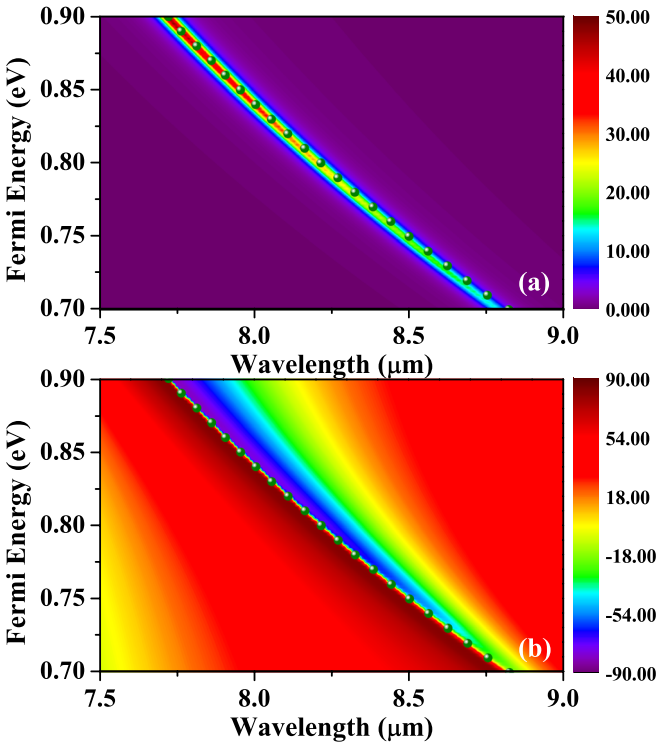

FIG. 3. (a) Calculated amplitude ratio and (b) phase difference between two orthogonal polarization states as a function of Fermi energy and wavelength. The olive balls indicate that the reflection phase difference is 0°.

equation $k_{spp} = \hbar\omega^2/(2\alpha_0 E_F c)$,[27] the resonant wavelength can be written as $\lambda_R \propto \sqrt{2\pi^2\hbar c L_{eqv}/(\alpha_0 E_F)} \propto \sqrt{L_{eqv}/E_F}$, where α_0 is the fine structure constant. The resonant wavelength λ_R is determined by the equivalent resonant length and Fermi energy of *L*-shaped graphene nanostructure. Hence, graphene polarization converter is more active than metallic one, since it can be tuned only by changing the Fermi energy without reoptimizing the geometrical parameters. It may find numerous applications in compact elements, such as tunable polarizers and polarization switchers.

To demonstrate the tunable broadband CPC of our designed graphene metamaterial, we calculated the reflectance and phase difference between *x* and *y* components as Fermi energy gradually varies from 0.7 eV to 0.9 eV. The wavelength at which the reflection phase difference is 0° was extracted from different Fermi energies. The corresponding PCR, polarized reflectances R_{xy}, and polarization azimuth angle θ at every wavelength, where the reflectance phase difference is 0°, are calculated in Fig. 4. By changing the Fermi energy from 0.7 eV to 0.9 eV, the PCR and the polarization azimuth angle θ are larger than 0.93 and 88.8° within a wide wavelength range from 7.7 μm to 8.8 μm, respectively, which demonstrate the tunable broadband CPC from *x* to *y* directions. In addition, the polarized reflectances R_{xy} is above 62% within a broad wavelength range. It indicates that the high efficient broadband CPC with high reflectance can be achieved only by tuning the Fermi energy of graphene, without extending the operation bandwidth at the cost of reflectance attenuation by conventionally stacking of different wave plates and system optimizing.

On the other hand, this characteristic of tunable CPC can be efficiently utilized as the mechanism to achieve

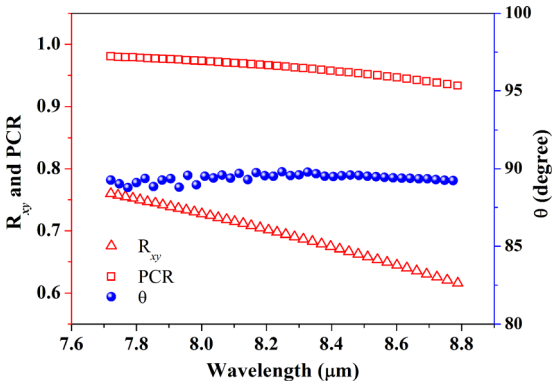

FIG. 4. Calculated corresponding PCR, polarized reflectances R_{xy}, and polarization azimuth angle θ at every wavelength, where the reflection phase difference is 0°.

polarization switch by tuning the Fermi energy in the broadband mid-IR wavelengths. Figure 5 shows the reflectance in two orthogonal polarization states with *x*-polarization incidence and PCR as a function of Fermi energy, where the incident wavelength is fixed at 8.2 μm. Figure 5(a) shows that the reflected wave is dominated by *x* polarized component, when the Fermi energy is 0.7 eV. The polarization of incident wave has not apparently changed. However, when the Fermi energy is increased to 0.8 eV, the reflected wave is dominated by *y* polarized component, which converts the incident wave to its cross polarization with PCR of 96% (see in Fig. 5(b)). The conversion from *x* to *y* polarization at wavelength 8.2 μm can be switched between 0% and 96% by simply varying the Fermi energy with an amount of $\Delta E_F = 0.1$ eV. The proposed polarization switch can also be achieved at other wavelengths by changing the Fermi energy of the designed tunable CPC.

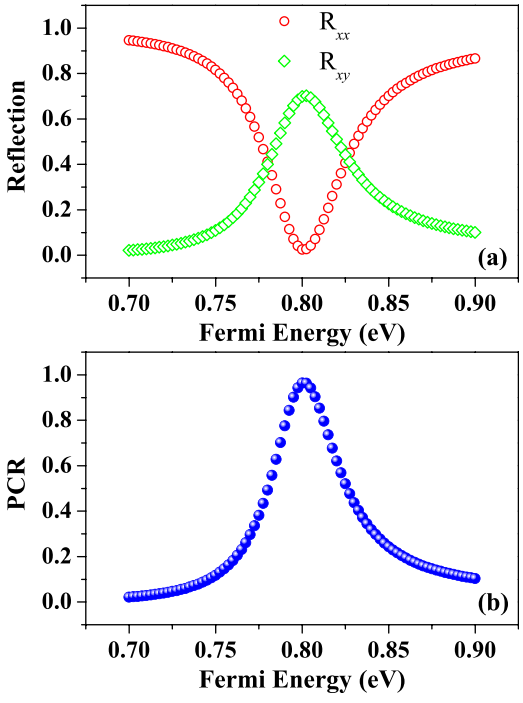

FIG. 5. (a) Calculated polarized reflectances R_{xx} and R_{xy} in two orthogonal polarization states and (b) PCR as a function of Fermi energy, where the incident wavelength is fixed at 8.2 μm.

In conclusion, we have proposed a highly tunable optical CPC based on graphene-enabled metamaterial in the mid-IR regime. The proposed CPC can convert linearly polarized light to its cross polarization in the reflection mode. Moreover, the polarization conversion can be dynamically tuned and realize a broadband effect by varying the Fermi energy without reoptimizing the nanostructures or sacrificing the reflectance amplitude by conventional method of stacking different wave plates. It can also realize the applications as tunable polarizers and polarization switchers. We believe this designed method may have applications in many areas like optics, analytical chemistry, and molecular biology and can be generalized to other frequency regimes such as THz and even the microwave regimes.

This work was supported by the National Basic Research Program (973 Program) of China (2012CB921900), the Chinese National Key Basic Research Special Fund (2011CB922003), the Natural Science Foundation of China (11304163, 61378006 and 61008002), the Program for New Century Excellent Talents in University (NCET-13-0294), the Natural Science Foundation of Tianjin (13JCQNJC01900), the Specialized Research Fund for the Doctoral Program of Higher Education (20120031120032 and 20100031120005), and the 111 project (B07013).

[1]A. Lakhtakia, *Selected Papers on Natural Optical Activity* (SPIE Press, Bellingham, WA, 1990).
[2]Z. Marcet, H. B. Chan, D. W. Carr, J. E. Bower, R. A. Cirelli, F. Klemens, W. M. Mansfield, J. F. Miner, C. S. Pai, and I. I. Kravchenko, Appl. Phys. Lett. **98**, 151107 (2011).
[3]Y. Ye and S. He, Appl. Phys. Lett. **96**, 203501 (2010).
[4]J. Han, H. Li, Y. Fan, Z. Wei, C. Wu, Y. Cao, X. Yu, F. Li, and Z. Wang, Appl. Phys. Lett. **98**, 151908 (2011).
[5]L. Cong, W. Cao, X. Zhang, Z. Tian, J. Gu, R. Singh, J. Han, and W. Zhang, Appl. Phys. Lett. **103**, 171107 (2013).
[6]T. Li, S. M. Wang, J. X. Cao, H. Liu, and S. N. Zhu, Appl. Phys. Lett. **97**, 261113 (2010).
[7]F. I. Baida, M. Boutria, R. Oussaid, and D. Van Labeke, Phys. Rev. B **84**, 035107 (2011).
[8]Z. H. Zhu, C. C. Guo, K. Liu, W. M. Ye, D. Yuan, B. Yang, and T. Ma, Opt. Lett. **37**, 698 (2012).
[9]N. K. Grady, J. E. Heyes, D. Roy Chowdhury, Y. Zeng, M. T. Reiten, A. K. Azad, A. J. Taylor, D. A. R. Dalvit, and H. Chen, Science **340**, 1304 (2013).
[10]J. Xu, T. Li, F. F. Lu, S. M. Wang, and S. N. Zhu, Opt. Express **19**, 748 (2011).
[11]Z. Wei, Y. Cao, Y. Fan, X. Yu, and H. Li, Appl. Phys. Lett. **99**, 221907 (2011).
[12]C. Wu, H. Li, X. Yu, F. Li, H. Chen, and C. T. Chan, Phys. Rev. Lett. **107**, 177401 (2011).
[13]S. Khatua, W. Chang, P. Swanglap, J. Olson, and S. Link, Nano Lett. **11**, 3797 (2011).
[14]N. Shen, M. Massaouti, M. Gokkavas, J. Manceau, E. Ozbay, M. Kafesaki, T. Koschny, S. Tzortzakis, and C. M. Soukoulis, Phys. Rev. Lett. **106**, 037403 (2011).
[15]A. A. Zharov, I. V. Shadrivov, and Y. S. Kivshar, Phys. Rev. Lett. **91**, 037401 (2003).
[16]S. Thongrattanasiri, F. H. L. Koppens, and F. Javier García de Abajo, Phys. Rev. Lett. **108**, 047401 (2012).
[17]C. Chen, C. Park, B. W. Boudouris, J. Horng, B. Geng, C. Girit, A. Zettl, M. F. Crommie, R. A. Segalman, S. G. Louie, and F. Wang, Nature **471**, 617 (2011).
[18]Z. Zeng, X. Huang, Z. Yin, H. Li, Y. Chen, H. Li, Q. Zhang, J. Ma, F. Boey, and H. Zhang, Adv. Mater. **24**, 4138 (2012).
[19]A. Vakil and N. Engheta, Science **332**, 1291 (2011).
[20]S. H. Mousavi, I. Kholmanov, K. B. Alici, D. Purtseladze, N. Arju, K. Tatar, D. Y. Fozdar, J. Won Suk, Y. Hao, A. B. Khanikaev, R. S. Ruoff, and G. Shvets, Nano Lett. **13**, 1111 (2013).
[21]Z. Fang, S. Thongrattanasiri, A. Schlather, Z. Liu, L. Ma, Y. Wang, P. M. Ajayan, P. Nordlander, N. J. Halas, and F. Javier García de Abajo, ACS Nano **7**, 2388 (2013).
[22]A. Fallahi and J. Perruisseau-Carrier, Phys. Rev. B **86**, 195408 (2012).
[23]H. Cheng, S. Chen, P. Yu, J. Li, L. Deng, and J. Tian, Opt. Lett. **38**, 1567 (2013).
[24]H. Yan, X. Li, B. Chandra, G. Tulevski, Y. Wu, M. Freitag, W. Zhu, P. Avouris, and F. Xia, Nat. Nanotechnol. **7**, 330 (2012).
[25]Q. Bao, H. Zhang, B. Wang, Z. Ni, C. H. Y. X. Lim, Y. Wang, D. Y. Tang, and K. P. Loh, Nat. Photonics **5**, 411 (2011).
[26]M. A. Ordal, L. L. Long, R. J. Bell, S. E. Bell, R. R. Bell, R. W. Alexander, and C. A. Ward, Appl. Opt. **22**, 1099 (1983).
[27]F. H. L. Koppens, D. E. Chang, and F. Javier García de Abajo, Nano Lett. **11**, 3370 (2011).
[28]K. S. Novoselov, A. K. Geim, S. V. Morozov, D. Jiang, Y. Zhang, S. V. Dubonos, I. V. Grigorieva, and A. A. Firsov, Science **306**, 666 (2004).
[29]COMSOL Multiphysics User's Guide, Version 3.5 (Comsol AB, Brulington, MA, 2008).
[30]J. M. Hao, Y. Yuan, L. X. Ran, T. Jiang, J. A. Kong, C. T. Chan, and L. Zhou, Phys. Rev. Lett. **99**, 063908 (2007).
[31]J. D. Jackson, *Classical Electrodynamics* (Wiley, New York, 1999).